

Diagnostic and Correction of Phase Aberrations in Scanning Transmission Microscopy by Artificial Neural Networks

Giovanni Bertoni^{1*}, Enzo Rotunno¹, Daan Marsmans², Peter Tiemeijer² and Vincenzo Grillo¹

¹ Istituto Nanoscienze, Consiglio Nazionale delle Ricerche, Modena, Italy.

² Thermo Fisher Scientific, Eindhoven, Netherlands.

* Corresponding author: giovanni.bertoni@cnr.it

The ultra-high-resolution of state-of-the-art scanning transmission microscopy (STEM) resides in the ability to correct aberrations of the probe forming lenses. In this way, atomically resolved images with Z-sensitive contrast can be obtained. The idea in this contribution is to test AI methods (artificial neural networks or ANN) to measure the aberrations from a *single* image of the stationary probe on an amorphous region, or Ronchigram intensity $I(q)$. The aim is to assist the microscopist in his manual tuning or to improve the existing routines available with probe correctors with faster ones. This will contribute in the pursuit of a fully automated alignment of the microscope, permitting the microscopist to focus on the properties of the sample in his research rather than spend time in technical procedures of alignment of the instrument itself. Recent approaches with deep learning techniques were demonstrated to be promising in optimizing the STEM aperture for improving resolution [1,2].

The intensity $I(q)$ of the Ronchigram image in reciprocal space (or frequency domain) can be written as:

$$I(q) = |\Psi(q)|^2 = |FT(IFT\{e^{-i\chi(q)}\}e^{-i\sigma V(x)})|^2,$$

where $\chi(q)$ is the phase due to the aberrations, $V(x)$ is the sample inner potential, σ is the interaction constant, and FT or IFT indicate the direct or inverse Fourier transforms, respectively. In our study, we have built a dataset of 20k images with different aberrations values. These were suitably patterned and passed to the ANN for the training (see Figure 1). The ANN is a custom VGG16 consisting of 2D convolution layers followed by 2D pooling and dropout layers, before the final flatten layers for the output. For demonstration purposes, we limited our study to the principal aberrations: defocus (C_1), two-fold astigmatism (A_1), coma (B_2), three-fold astigmatism (A_2) and spherical aberration (C_3). The predicted errors in the measured aberrations were obtained as mean absolute errors (MAE) from the entire set of input images, and from freshly generated datasets, confirming the ANN has reached a good performance, with a relative error $\sim 5\%$ with respect to the aberrations range limits.

An example of the successful ANN correction on synthetic images is shown in Figure 2, by comparing an image from the uncorrected probe (a), with the one obtained after ANN measurement and correction (b). The improved resolution is evident, and can be calculated by using the quarter-wave criterion and the circle with minimum radius (see blue circles) which determines the STEM aperture of semi-angle for optimal resolution $\alpha = \min(|\chi(q)| \leq \pi/4)$. The spatial resolution can be estimated from the Rayleigh criterion as $0.61(\lambda/\alpha)$, giving an improvement in this example from $\sim 4 \text{ \AA}$ to 0.6 \AA .

However, the effectiveness of the ANN prediction on real experiments is related to the accuracy of the model in describing the experimental images. In this contribution we will focus on:

- Compressing/patterning the Ronchigram images [3] to build an optimized ANN input.
- Defining a simple but realistic model of the sample potential $V(x)$ which is usually treated as a noise grating [4].
- Including the detector effects (point spread function and counting noise) [5].

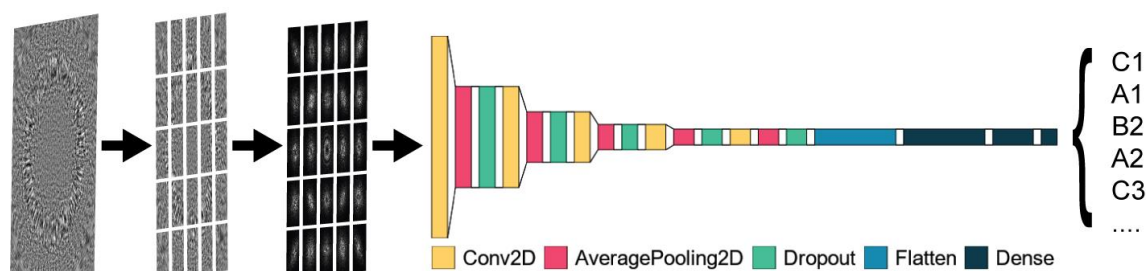


Figure 1. Schematic view of the process of ANN fitting of $I(q)$ Ronchigram images. We limited our study to main aberration values (C_1 , A_1 , B_2 , A_2 , C_3). Higher order aberrations up to 5th order were randomly generated as residual aberrations.

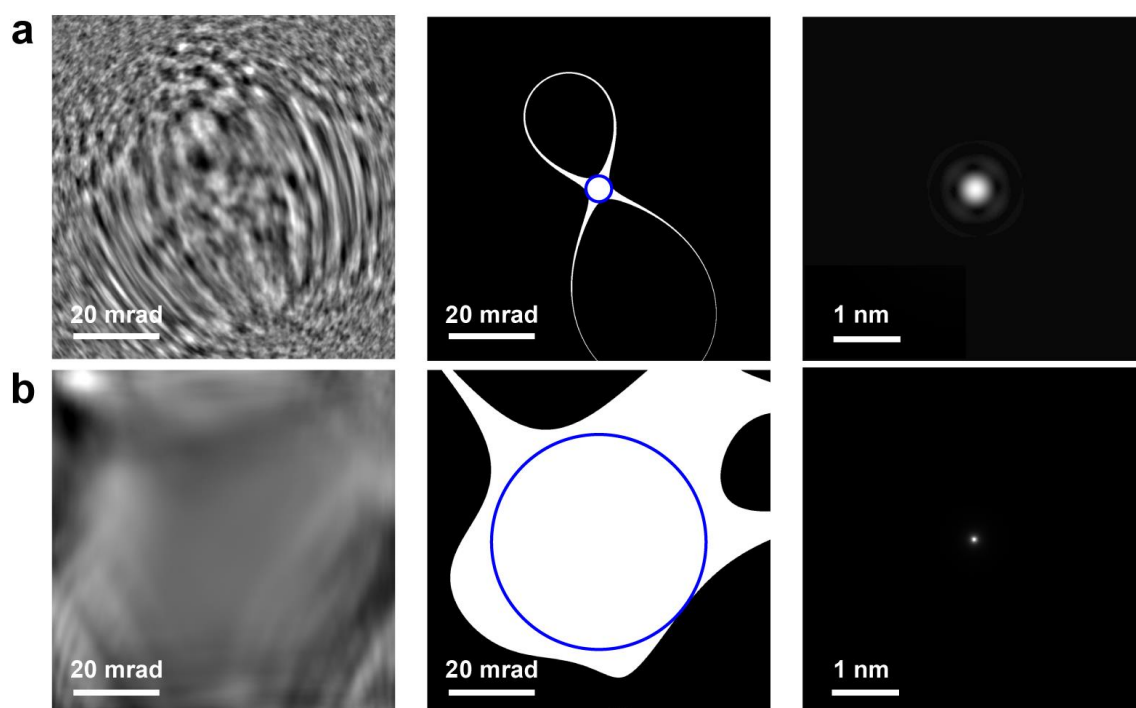


Figure 2. Simulated images to illustrate ANN correction capability. (a) Uncorrected probe. (b) Corrected probe after subtraction of the aberration values measured by the ANN. The Ronchigram intensity $I(q)$ images (left) and corresponding $|\chi(q)| \leq \pi/4$ mask (center) are calculated at defocus $C_1 = 0$ nm. The blue circle is the optimal probe aperture used to estimate the resolution from the Rayleigh criterion. (right) Corresponding probe image as calculated in vacuum.

References:

- [1] C Zhang et al., *Microscopy & Microanalysis* **27** (2021) doi:10.1017/S1431927621003214
- [2] N Schnitzer et al., *Microscopy & Microanalysis* **26** (2020), p. 921-928.
doi:10.1017/S1431927620001841
- [3] AR Lupini et al., *Ultramicroscopy* **110** (2010), p. 891-898. doi:10.1016/j.ultramic.2010.04.006
- [4] N Schnitzer et al., *Microscopy Today* **27** (2019), p. 12-15. doi:10.1017/S1551929519000427
- [5] The authors acknowledge funding from the European Union's Horizon 2020 Research and Innovation Programme under Grant Agreement No 964591 'SMART-electron'.